

# Magnetically tunable slow light based on alternative-row-elliptical-hole photonic crystal waveguide infiltrated with magnetic fluids

DELONG SU<sup>a</sup>, SHENGLI PU<sup>a,b\*</sup>, WEIZHENG LEI<sup>a</sup>

<sup>a</sup>College of Science, University of Shanghai for Science and Technology, Shanghai 200093, China

<sup>b</sup>Shanghai Key Laboratory of Modern Optical System, University of Shanghai for Science and Technology, Shanghai 200093, China

A kind of W1 line-defect waveguide based on alternative-row-elliptical-hole photonic crystal with triangular lattice is proposed for compact and high-performance slow light applications. The elliptical air-holes are infiltrated with magnetic fluids to realize the on-line tunable slow light. The plane-wave expansion method is employed to investigate the slow light properties numerically. The ultralow dispersion criterion is employed to evaluate the slow light performance. Through varying the major and minor axes of the elliptical air-holes, the optimized structure with high performance of slow light is obtained. The average group index decreases from 13.70 to 13.31 and the normalized delay bandwidth product increases from 0.524 to 0.544 when the magnetic field factor  $\alpha_{\parallel}$  changes from 0 to 1. The corresponding wavelength bandwidth  $\Delta\lambda$  centering at  $\lambda_0 = 1550$  nm varies from 59.26 to 63.33 nm.

(Received March 18, 2016; accepted June 09, 2016)

**Keywords:** Elliptical-hole, Photonic crystal waveguide, Tunability, Slow light, Magnetic fluid

## 1. Introduction

Recently, slow light in photonic crystal waveguide (PCW) [1] has attracted considerable interest for its promising applications, such as optical buffering [2, 3], optical modulation [4, 5], and nonlinearity enhancement for all-optical signal processing [6, 7]. Removing a row of holes/rods of an otherwise perfect two-dimensional (2-D) planar photonic crystal (PC) will form the W1 PCW, which has been studied extensively among all kinds of PCW devices [8, 9]. The group velocity dispersion (GVD) and normalized delay bandwidth product (NDBP) are the key parameters to evaluate the slow light performance. Usually, by changing the width of the line-defect [10, 11] or altering the air-hole radius/position of the first two rows adjacent to the line-defect [12-16], the slow light performance can be optimized.

The on-line tunability is most favorable for many pragmatic applications. As for the slow light devices, the on-line tunability can be realized by adjusting the external stimuli (such as electric field or magnetic field), which is assigned to the stimulus-dependent refractive index of constituent materials. Magnetic fluid (MF) is a kind of colloidal materials with excellent concentration- and

magnetic-field-dependent refractive index. It has been proved to have versatile optical properties and applications [17-23]. Consequently, MF may be a suitable candidate for enabling on-line tunable slow light. Besides, on-line tunable slow light with PC structures is very favorable for many practical applications and has gotten particular attention [24-27].

However, most of the proposed tunable PC slow light structures are based on circular air-hole PCWs. In this work, the traditional circular air-holes are replaced with elliptical holes to constitute the W1 PCWs. In addition, elliptical holes will be infiltrated with MFs, whose refractive indices can be adjusted by external magnetic field and the volume fraction of magnetic nanoparticles [28, 29]. This kind of magnetically controllable optical component has been proved feasible in 2-D model [30-32] and PC slab configuration [33]. But the employed PCWs are all based on circular air-holes. Through optimizing the major and minor axes of the elliptical holes, the alternative-row-elliptical-hole-based W1 PCW slow light structure with optimal slow light performance is designed. Besides, the slow light performance of the corresponding MF-infiltrated structure is further tuned on-line by the externally magnetic field.

## 2. Waveguide model and method

The proposed structure is PC slab with alternative-row-elliptical air-holes arrayed in a triangular pattern, which is schematically depicted in Fig. 1. The x-axis is parallel to the line-defect and the y-axis is perpendicular to the line-defect. The lattice constant is  $a$ . For the odd rows, the major and minor axes of the elliptical air-holes are along the x-axis and y-axis, respectively. Their lengths are labeled as  $D_x$  and  $D_y$ , respectively. While for the even rows, the major and minor axes of the elliptical air holes are along the y-axis and x-axis, respectively. Their lengths are labeled as  $D'_x$  and  $D'_y$ , respectively. In this work, the uniform elliptical hole is considered (i.e.  $D'_x = D_y$  and  $D'_y = D_x$ ). The optimization procedure consists in properly adjusting  $D_x$  and  $D_y$ . The waveguide layer is made of silicon with refractive index of 3.48. The substrate is made of silica with a refractive index of 1.45. The superstratum is air with a refractive index of 1. The silicon layer of SOI wafer has a thickness of  $h=283$  nm (same as that in Refs. 15 and 16). The air and silica layers are semi-infinite. For the magnetically tunability investigation, the elliptical holes are infiltrated with MF. The refractive index of infiltrated MF can be changed by adjusting the applied external magnetic field strength. Then, the tunable slow light properties for the proposed infiltrated structure can be realized.

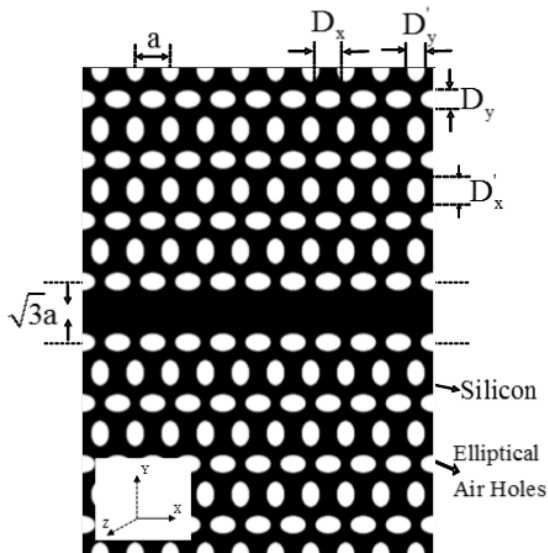


Fig. 1. Schematic of the line-defect W1 PCW with alternative-row-elliptical air-holes.

To investigate the band structures and dispersion properties of the designed PC and corresponding W1 waveguide, the MIT Photonic Bands Package based on

plane-wave expansion method is adopted. Due to the time-consuming nature of three dimensional (3-D) calculations, the 2-D analysis with an equivalent slab effective index of 3.0095 for TE modes (electrical field lies in the slab plane) is adopted [33]. According to Ref. 33, the initial major and minor axes are set at  $D_x = D_y = 0.60a$  in this work. The corresponding dispersion diagram is shown in Fig. 2, where the wave vector has been normalized to  $2\pi/a$ , i.e.  $k_N = ka/(2\pi)$ . The ordinate in Fig. 2 denotes frequency, which has been normalized to  $2\pi c/a$  ( $c$  is the light speed in vacuum) and equals  $a/\lambda$ , i.e.  $\omega_N = \omega a/(2\pi c) = a/\lambda$ . Fig. 2 indicates that the designed W1 PCW supports even and odd modes within the photonic band gap (PBG). The even PBG mode tends to flatten at large wave vector, which is due to the folding at the Brillouin zone edge. This is favorable for obtaining slow light with high group index. Therefore, the slow light properties of even mode will be investigated in detail hereafter.

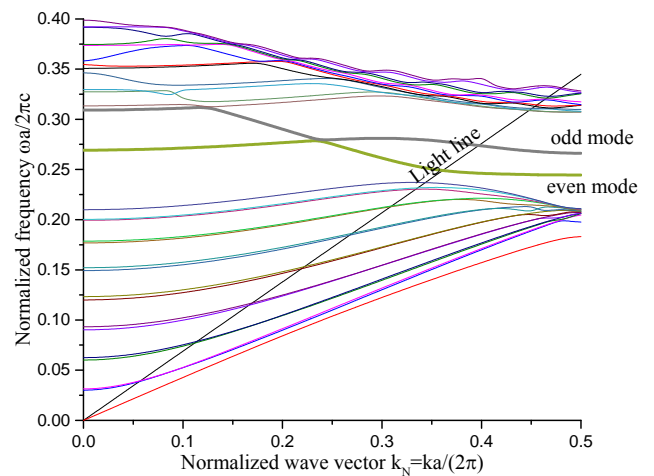


Fig. 2. Typical projected band dispersion diagram of the line-defect W1 PCW with alternative-row-elliptical air-holes.

In order to optimize the slow light performance of the proposed structure, the major and minor axes of elliptical holes are adjusted while the filling factor of air-hole is kept unchanged. The filling factor of air-hole is defined as  $f = S_{\text{hole}}/S_{\text{lattice}}$ , where  $S_{\text{hole}}$  is the area occupied by the hole within an area of  $S_{\text{lattice}}$ . Therefore, for the initial elliptical air-hole structure with  $D_x = D_y = 0.60a$ , the filling factor for all structures is fixed at 0.3265. The different sets of major and minor axes of elliptical holes are listed in Table 1.

Table 1. Different major and minor axes of elliptical air-hole (The filling factor is kept at 0.3265).

Structure number	1	2	3	4	5
$D_x$	0.50a	0.55a	0.60a	0.65a	0.72a
$D_y$	0.72a	0.65a	0.60a	0.55a	0.50a

For investigating the on-line magnetically tunable slow light properties of the MF-infiltrated W1 PCW, the Maxwell-Garnett approximation is utilized to get the magnetic-field-dependent effective dielectric constant  $\epsilon_{MF}$  of MF, which can be expressed as [34-36]

$$\frac{\epsilon_{MF} - \epsilon_{liq}}{\alpha_{||} \epsilon_{MF} + (3 - \alpha_{||}) \epsilon_{liq}} = \phi \frac{\epsilon_{particle} - \epsilon_{liq}}{\epsilon_{particle} + 2\epsilon_{liq}}, \quad (1)$$

where  $\epsilon_{liq}$  and  $\epsilon_{particle}$  are the dielectric constants of the carrier liquid and nanoparticles, respectively.  $\phi$  is the

volume fraction of magnetic nanoparticles within the MF. The parameter  $\alpha_{||}$  measures the degree of externally-magnetic-field-induced structural anisotropy (nanoparticle chain formation). It is the local magnetic field factor for the longitudinal configuration, i.e. the E-component of the incident electromagnetic wave is parallel to the nanoparticle chain induced by the externally applied magnetic field. The value of  $\alpha_{||}$  lies in the range of  $0 < \alpha_{||} < 1$  and is inversely proportional to the strength of externally applied magnetic field. Therefore,  $\alpha_{||} = 1$  corresponds to zero magnetic field while  $\alpha_{||} = 0$  means infinite magnetic field. In this work,  $\epsilon_{liq} = 1.448^2$  [37] and  $\epsilon_{particle} = 2.2^2$  [38] are considered. As an example,  $\phi = 0.5$  is adopted. According to Eq. (1), the local magnetic field factor (i.e. magnetic field strength) dependent refractive index of MF is obtained and tabulated in Table 2.

Table 2. Refractive index of magnetic fluid at different local magnetic field factors.  $\epsilon_{liq} = 1.448^2$ ,  $\epsilon_{particle} = 2.2^2$ , and  $\phi = 0.5$ .

Local magnetic field factor $\alpha_{  }$	0	0.2	0.4	0.6	0.8	1
Refractive index $\sqrt{\epsilon_{MF}}$	1.7469	1.7555	1.7645	1.7741	1.7843	1.7952

### 3. Results and discussion

Using the data in Table 1, the projected band dispersion diagrams of the designed W1 PCWs with alternative-row-elliptical air-holes unfilled with MFs are calculated out. The corresponding results are shown in Fig. 3. The left inset of Fig. 3 is the actual calculation supercell for the equivalent 2-D calculation method. The supercell has 1 unit in the x direction and 8 units in the y direction. The resolution used for both directions is 32 grid points per unit cell. The silica light line is also shown. Light can only propagate within the waveguide for the frequency under the light line.

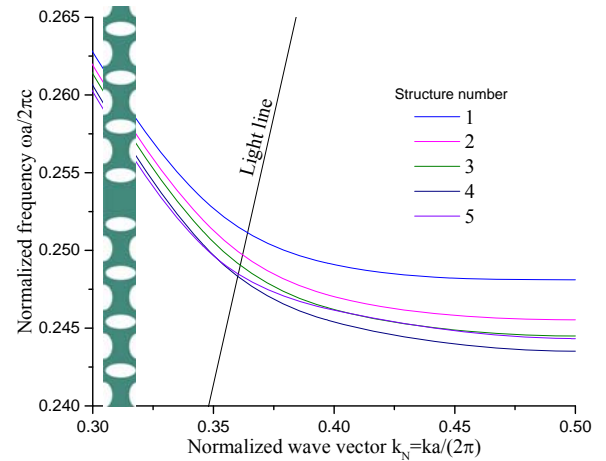


Fig. 3. Projected band dispersion diagrams of the unfilled W1 PCW with various sets of major and minor axes of elliptical holes. The supercell used for calculation is shown in the inset.

According to the projected band dispersion diagrams, both of the group index  $n_g = c \frac{dk}{d\omega} = \frac{dk_N}{d\omega_N}$  and GVD

$\beta_2 = \frac{d^2k}{d\omega^2} = \frac{1}{c} \frac{dn_g}{d\omega} = \frac{a}{2\pi c^2} \frac{dn_g}{d\omega_N}$  are calculated out. The

corresponding results are illustrated in Figs. 4 and 5, respectively. Fig. 5 only shows the ultralow-dispersion regime, i.e. the absolute value of GVD  $\beta_2$  is smaller than  $1 \times 10^4 a / (2\pi c^2)$ , which is two orders of magnitude smaller than that utilized in other works [39, 40].

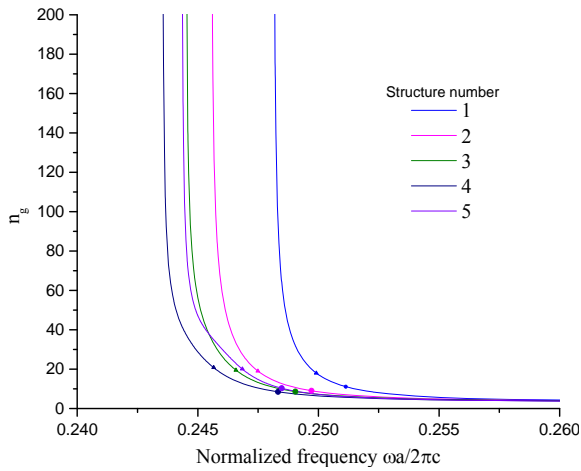


Fig. 4. Group index of even PBG mode of the unfilled W1 PCW with various sets of major and minor axes of elliptical holes.

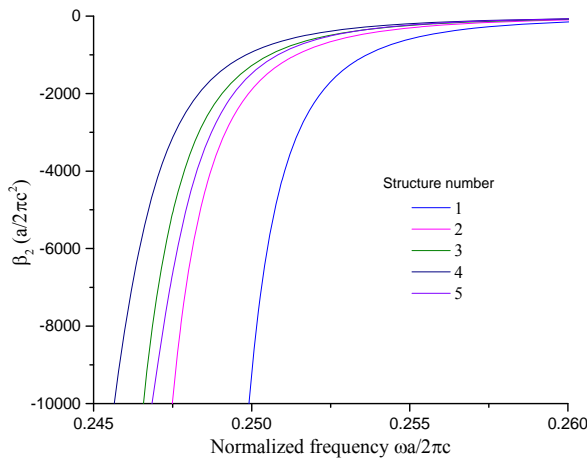


Fig. 5. GVD of even PBG mode of the unfilled W1 PCW with various sets of major and minor axes of elliptical holes.

For quantifying and comparing the slow light performance of different structures, the normalized delay-bandwidth product  $NDBP = \tilde{n}_g \times \frac{\Delta\omega}{\omega_0} = \tilde{n}_g \times \frac{\Delta\omega_N}{\omega_{N0}}$  is employed, where  $\tilde{n}_g$  is the average group index within the bandwidth  $\Delta\omega_N$  and  $\omega_{N0}$  is center frequency. There are two different criteria to determine the bandwidth  $\Delta\omega_N$

[41]. The first is called *low dispersion criterion*, which is based on the dispersion variation range, leading to estimation of the frequency bandwidth by considering the dispersion parameter  $\beta_2$  with absolute value lower than  $1 \times 10^4 a / (2\pi c^2)$  (ultralow-dispersion criterion). The second one is called *constant group index criterion*, which consists in evaluating the frequency bandwidth corresponding to a maximum of  $\pm 10\%$   $n_g$  variation with respect to the average group index  $\tilde{n}_g$ .

In this work, the ultralow dispersion criterion is utilized. So, the highest acceptable frequencies  $\omega_{NH}$  are those cross the silica light line in Fig. 3 and the lowest ones  $\omega_{NL}$  correspond to the abscissa intercepts of the dispersion curves in Fig. 5. Therefore, the bandwidth  $\Delta\omega_N = \omega_{NH} - \omega_{NL}$ , central frequency  $\omega_{N0} = (\omega_{NH} + \omega_{NL})/2$ , and then the normalized bandwidth  $\Delta\omega_N/\omega_{N0}$  are easily obtained. Using  $\omega_{NH}$ ,  $\omega_{NL}$  and  $\omega_{N0}$ , the corresponding minimum, maximum and average group index ( $n_{g\min}$ ,  $n_{g\max}$ ,  $\tilde{n}_g$ ) are achieved from Fig. 4. Based on these methods, the average group index  $\tilde{n}_g$ , normalized bandwidth  $\Delta\omega/\Delta\omega_0$  and NDBP of our designed unfilled W1 PCW structures with alternative-row-elliptical air-holes are plotted in Fig. 6.

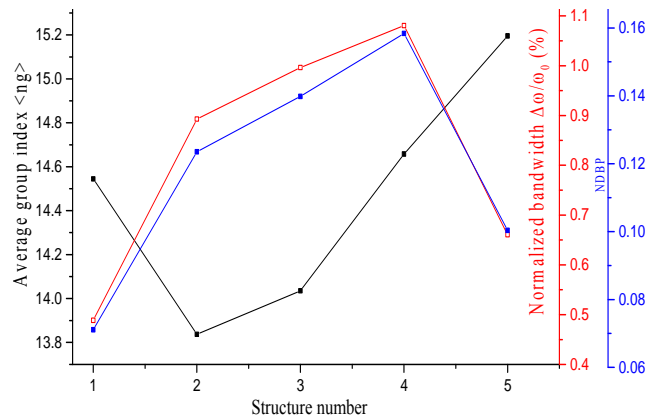


Fig. 6. Average group index, normalized bandwidth, and NDBP of the unfilled W1 PCW with various sets of major and minor axes of elliptical holes.

Fig. 6 shows that the structure with  $D_x = 0.65a$  and  $D_y = 0.55a$  (structure number 4) has a maximum NDBP of 0.1584. The corresponding average group index and normalized bandwidth are 14.658 and 1.081%,

respectively. Thereafter, this optimized structure is chosen to investigate the on-line magnetically tunability of slow light performance.

Using the data in Table 2, the tunable slow light performance of the optimized alternative-row-elliptical holes PCW structure ( $D_x = 0.65a$  and  $D_y = 0.55a$ ) infiltrated with MFs are investigated. The corresponding group indices as a function of frequency for magnetic field factor  $\alpha_{||}$  varying from 0 to 1 are shown in Fig. 7. For comparison, the result for the corresponding unfilled PCW is also plotted. It is obvious from Fig. 7 that MF-infiltration can considerably change the group index, which can be further tuned on-line by changing the magnetic field strength.

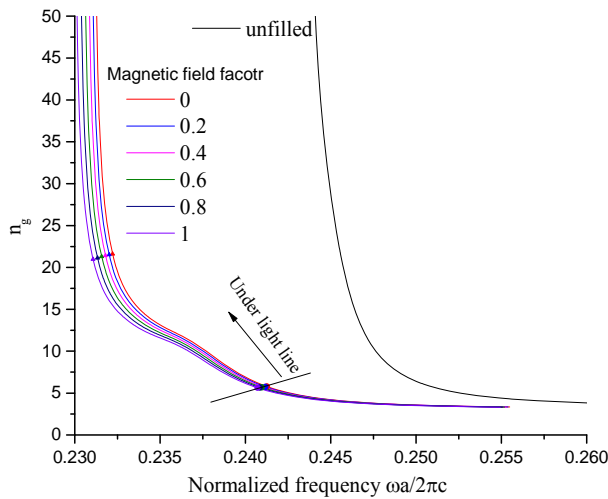


Fig. 7. Group index as a function of frequency at different magnetic field factors  $\alpha_{||}$  for the alternative-row-elliptical air-hole PCW infiltrated with MFs. The result of the corresponding unfilled PCW is also plotted for comparison.

Using the above-mentioned methods, the relationship between average group index  $\tilde{n}_g$  (or normalized bandwidth  $\Delta\omega/\omega_{N0}$ , or NDBP) and magnetic field factor  $\alpha_{||}$  is plotted in Fig. 8. Fig. 8 shows that the average group index  $\tilde{n}_g$  decreases linearly with the magnetic field factor  $\alpha_{||}$ , while the normalized bandwidth  $\Delta\omega/\omega_{N0}$  and NDBP increase linearly with the magnetic field factor  $\alpha_{||}$ . The average group index can be tuned with the magnetic field factor in the range of 13.70-13.31. The normalized bandwidth and NDBP can be tuned with the magnetic field factor in the range of 3.823-4.086% and 0.524-0.544, respectively. Hence, the wavelength bandwidth  $\Delta\lambda$  centering at  $\lambda_0 = 1550$  nm varies from

59.26 to 63.33 nm when the magnetic field factor  $\alpha_{||}$  changes from 0 to 1. The achieved slow light performances are superior to those of our previous designed structure, which is based on the W0.9 PCW with circular holes arrayed in triangular pattern [33].

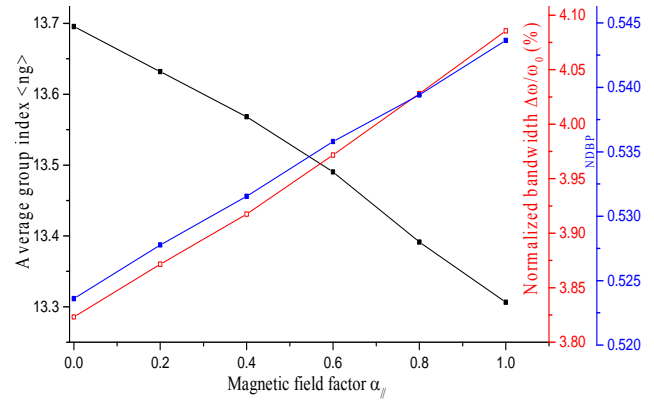


Fig. 8. Average group index, normalized bandwidth and NDBP as functions of magnetic field factor for the alternative-row-elliptical air-hole PCW infiltrated with MFs.

#### 4. Conclusions

In summary, the W1 PCW with MF-infiltrated alternative-row-elliptical air-holes arrayed in a triangular pattern is designed. The effective refractive index method based on 2-D plane-wave expansion calculation is employed to investigate the slow light properties. The ultralow dispersion criterion is utilized to study the slow light performance. The initial lengths of major and minor axes of elliptical holes are selected at  $0.60a$ . Through adjusting the major and minor axes of elliptical holes while keeping the filling factor of air-hole unchanged, the optimized structure parameter is found to be  $D_x = 0.65a$  and  $D_y = 0.55a$ . For the optimized slow light structure, the average group index  $\tilde{n}_g$  can be tuned from 13.70 to 13.31 with the magnetic factor  $\alpha_{||}$  varying from 0 to 1. The corresponding normalized bandwidth and NDBP can be tuned from 3.823 to 4.086% and from 0.524 to 0.544, respectively.

#### Acknowledgments

This research is supported by Natural Science Foundation of Shanghai (Grant No. 13ZR1427400), Shanghai Talent Development Fund (Grant No. 201529), Shanghai Key Laboratory of Specialty Fiber Optics and Optical Access Networks (Grant No. SKLSFO2014-05) and Huijiang Foundation of China (Grant No. B14004).

## References

- [1] T. Baba, *Nat. Photonics*. **2**, 465 (2008).
- [2] F. Long, H. Tian, Y. Ji, *J. Lightwave Technol.* **28**, 1139 (2010).
- [3] Y. Zhai, H. Tian, Y. Ji, *J. Lightwave Technol.* **29**, 3083 (2011).
- [4] Y. A. Vlasov, M. O'Boyle, H. F. Hamann, S. J. McNab, *Nature*. **438**, 65 (2005).
- [5] X. Chen, Y. S. Chen, Y. Zhao, W. Jiang, R. T. Chen, *Opt. Lett.* **34**, 602 (2009).
- [6] R. Iliew, C. Etrich, T. Pertsch, F. Lederer, *Phys. Rev. B*. **77**, 115124 (2008).
- [7] T. F. Krauss, *Nat. Photonics*. **2**, 448 (2008).
- [8] M. Lončar, T. Doll, J. Vučković, A. Scherer, *J. Lightwave Technol.* **18**, 1402 (2000).
- [9] M. Notomi, K. Yamada, A. Shinya, J. Takahashi, C. Takahashi, I. Yokohama, *Phys. Rev. Lett.* **87**, 253902 (2001).
- [10] A. Y. Petrov, M. Eich, *Appl. Phys. Lett.* **85**, 4866 (2004).
- [11] F. Long, H. Tian, Y. Ji, *Appl. Opt.* **49**, 4808 (2010).
- [12] S. Kubo, D. Mori, T. Baba, *Opt. Lett.* **32**, 2981 (2007).
- [13] L. H. Frandsen, A. V. Lavrinenko, J. Fage-Pedersen, P. I. Borel, *Opt. Express*. **14**, 9444 (2006).
- [14] J. Li, T. P. White, L. O'Faolain, A. Gomez-Iglesias, T. F. Krauss, *Opt. Express*. **16**, 6227 (2008).
- [15] R. Hao, E. Cassan, H. Kurt, X. L. Roux, D. Marris-Morini, L. Vivien, H. Wu, Z. Zhou, X. Zhang, *Opt. Express*. **18**, 5942 (2010).
- [16] R. Hao, E. Cassan, X. L. Roux, D. Gao, V. D. Khanh, L. Vivien, D. Marris-Morini, X. Zhang, *Opt. Express*. **18**, 16309 (2010).
- [17] L. Luo, S. Pu, J. Tang, X. Zeng, M. Lahoubi, *Appl. Phys. Lett.* **106**, 193507 (2015).
- [18] J. Liu, Y. Mao, J. Ge, *J. Mater. Chem. C*. **1**, 6129 (2013).
- [19] R. Gao, Y. Jiang, S. Abdelaziz, *Opt. Lett.* **38**, 1539 (2013).
- [20] L. Gao, T. Zhu, J. Zeng, K. S. Chiang, *Appl. Phys. Express*. **6**, 052502 (2013).
- [21] V. Mahendran, J. Philip, *Appl. Phys. Lett.* **102**, 063107 (2013).
- [22] K. Kondo, M. Shinkawa, Y. Hamachi, Y. Saito, Y. Arita, T. Baba, *Phys. Rev. Lett.* **110**, 053902 (2013).
- [23] N. Ishikura, R. Hosoi, R. Hayakawa, T. Tamanuki, M. Shinkawa, T. Baba, *Appl. Phys. Lett.* **100**, 221110 (2012).
- [24] A. Casas-Bedoya, C. Husko, C. Monat, C. Grillet, N. Gutman, P. Domachuk, B. J. Eggleton, *Opt. Lett.* **37**, 4215 (2012).
- [25] M. Ebnali-Heidari, C. Grillet, C. Monat, B. J. Eggleton, *Opt. Express*. **17**, 1628 (2009).
- [26] H. E. Horng, C.-Y. Hong, S. Y. Yang, H. C. Yang, *Appl. Phys. Lett.* **82**, 2434 (2003).
- [27] H. Wang, S. Pu, N. Wang, S. Dong, J. Huang, *Opt. Lett.* **38**, 3765 (2013).
- [28] S. Pu, H. Wang, N. Wang, X. Zeng, *Appl. Phys. B*. **112**, 223 (2013).
- [29] O. Guillan-Lorenzo, and F. J. Diaz-Otero, *Opt. Commun.* **359**, 49 (2016).
- [30] N. Zhu, C. Chen, Y. Li, Z. Jiang, *J. Nanophoton.* **9**, 093045 (2015).
- [31] S. Pu, S. Dong, J. Huang, *J. Opt.* **16**, 045102 (2014).
- [32] C. Z. Fan, G. Wang, J. P. Huang, *J. Appl. Phys.* **103**, 094107 (2008).
- [33] J. P. Huang, K. W. Yu, *Phys. Rep.* **431**, 87 (2006).
- [34] C. Z. Fan, J. P. Huang, *Appl. Phys. Lett.* **89**, 141906 (2006).
- [35] [www.instant-analysis.com/Principles/refraction.htm](http://www.instant-analysis.com/Principles/refraction.htm).
- [36] U. Buchenau, I. Muller, *Solid State Commun.* **11**, 1291 (1972).
- [37] R. Hao, E. Cassan, H. Kurt, J. Hou, X. Leroux, D. Marris-Morini, L. Vivien, D. Gao, Z. Zhou, X. Zhang, *IEEE Photon. Technol. Lett.* **22**, 844 (2010).
- [38] J. Ma, C. Jiang, *IEEE Photon. Technol. Lett.* **20**, 1237 (2008).
- [39] Y. Xu, L. Xiang, E. Cassan, D. Gao, X. Zhang, *Appl. Opt.* **52**, 1155 (2013).
- [40] W. Lei, S. Pu, *J. Magn.* **20**, 110 (2015).

\*Corresponding author: shlpu@usst.edu.cn